RESEARCH PAPER

A comparative study of solid-silver and silver-shell nanodimers on surface plasmon resonances

Yuan-Fong Chau · Han-Hsuan Yeh

Abstract We investigated numerically the scattering cross sections and near-field intensities of solid-silver and silver-shell (shell thickness $d = 10$ nm) nanodimers that interact with incident plane wave by the use of finite-element method with three-dimensional models. Results show that the silver-shell cases exhibit tunable surface plasmon resonances and its rotational effects can induce more surface plasmons in a wider range of wavelength that are not observed for the solid-silver cases with the same volume (1,046,666 nm^3).

Introduction

Metal nanoshells are a new class of nanoparticles with highly tunable optical properties and plasmon resonance, allowing materials to be specially designed to match the wavelength required for a particular application. Metal nanoshells possess several attractive features which make them interesting as nanoscale optical components (Averitt et al. 1997; Chau et al. 2010).

Y.-F. Chau (✉) · H.-H. Yeh
Department of Electronic Engineering, Ching Yun University, Jung-Li, Taiwan 320, ROC
e-mail: yfc01@cyu.edu.tw

Experimentally, the first metal nanoshell, developed by Zhou et al. (1994), consists of an Au_2S dielectric core surrounded by a gold nanoshell. Several numerical studies of this phenomenon have been performed on different particle shapes (Kottmann et al. 2000) and particles surrounded by nanoshells (Prodan et al. 2003; Oubre and Nordlander 2005). Arrays of metallic nanoparticles are also used to transfer electromagnetic energy in the near-field regime (Quinten et al. 1998; Chen et al. 2009). However, the effects on various patterns of three-dimensional (3-D) metal-shell nanodimers have not been considered. In recent years, the physical and chemical properties of metallic nanoshells have received particular attention (Husu et al. 2008; Hu et al. 2009). They possess a plasmon-derived tunable optical resonance controlled by the dimensions of hollows in the nanodimer and the thickness of the metallic shell, spanning much of the visible and infrared regions of the optical spectrum (Hu et al. 2009).

In this paper, we study the light scattering cross sections (SCSs) and near-field intensities on various geometries of solid-silver and silver-shell nanodimer interacting with a transverse magnetic (TM)-mode incident plane wave in 3-D models using the finite-element method (FEM). The enclosure of a pair of nanodimer which electromagnetic field is effectively confined in the gap and the surface of the nanodimer can generate high local-field enhancement. We have compared the optical response in near-field zone of the solid-silver nanodimer with the silver-shell one. The influences of wavelength of incident light on

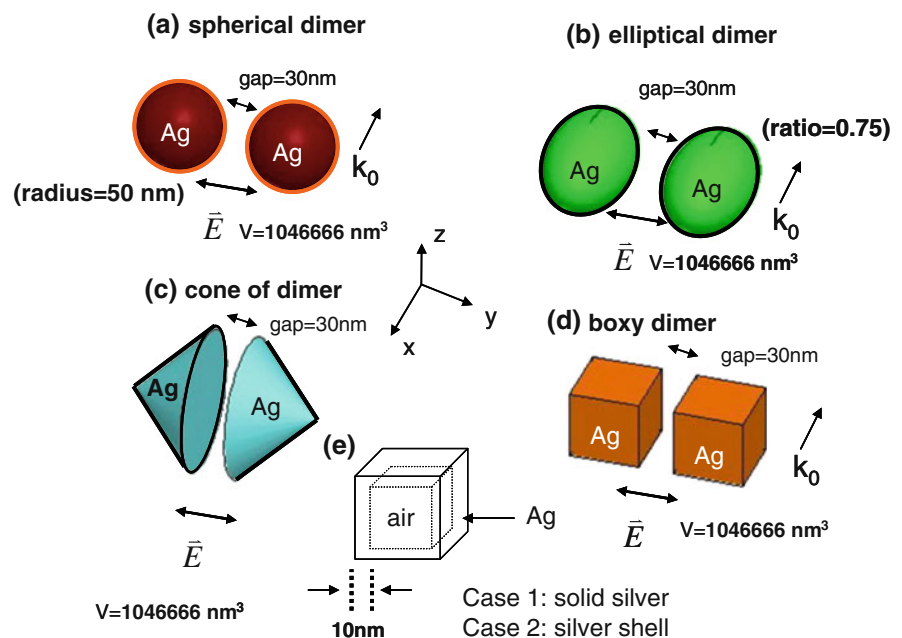local-field enhancement and red-shifting are discussed in our simulations.

Simulation models, method, results, and discussion

The dispersion properties of the metal must be considered here since the absorption and permittivity of the metallic material are frequency dependent. The Drude model is used to describe the dependence of the metallic permittivity on the frequency (Gresho and Sani 2000). The 3-D FEM that we applied to metal nanoparticles was comprehensively described in Gresho and Sani (2000). Silver permittivity data are obtained from Johnson and Christy (1972) and corrected with the Drude model, which includes the size effect (Okamoto and Kawata 2001). In our formulation we used triangular high order edge elements. To model an infinite simulation region with a 3-D finite-geometry model (i.e., to enclose the computational domain without affecting the numerical solution), it is necessary to use anisotropic perfectly matched layers (PMLs) (Gresho and Sani 2000) that are placed before the outer boundary. This formulation can be used to deal with anisotropic material in terms of both dielectric permittivity and magnetic permeability, allowing anisotropic PMLs to be implemented directly.

For nanoparticles with sizes down to the optical wavelength, the surface plasmon resonances (SPRs) are clearly dipolar and can be satisfactorily described by the lowest order of the series of spherical harmonics of Mie theory. For larger particles, typically in the 100 nm range, retardation effects inside the plasmonic particles lead to the appearance of higher order multipolar plasmon resonances that show off as new features in the optical spectra (Marty et al. 2010). SPRs are usually sensitive to different wavelengths of incident light. For a solid-silver nanoparticle, strong light absorbing and scattering occur at plasmon resonance frequency and high local fields were excited around the nanoparticle. However, in a system consisting of a pair of nanoparticles, the SPR condition is modified for particle–particle interaction and the absorption curve is broadened. It is necessary to investigate the wavelength-dependent responses of nanoparticle pair to understand the roles of surface plasmon effects and particle–particle interaction (Chau et al. 2008, 2007).

For convenience, we name the solid-silver nanodimer as case 1 and the silver-shell nanodimer as case 2 (see Fig. 1e). Four patterns, i.e., (a) spherical, (b) elliptical, (c) cone of and (d) boxy silver nanodimer with the same outer volumes $V = 1,046,666$ nm^3, are analyzed for comparison, as shown in Fig. 1a–d. We compare the SCSs and near-field optical response of case 1 with case 2, which are illuminated with a

Fig. 1 Four patterns of simulation models: **a** spherical, **b** elliptical, **c** cone of and **d** boxy silver-shell nanodimers with the same volumes $V = 1,046,666$ nm^3. **e** Schematic model of case 1 (solid nanodimer) and case 2 (shell-like nanodimer)

transverse magnetic (TM) incident plane wave and propagated in the $\bar{k}_0$ direction. The direction of the electric field $\bar{E}$ is perpendicular to $\bar{k}_0$ and parallel to the plane of incidence. The wavelength of incident light varies from 300 to 800 nm and the near-field intensity is measured in the central part of the gap (interparticle distance). The effect of gap should be considered and the gap is set to $g = 30$ nm based on our previous work (Chau et al. 2008).

Near-field intensities of local fields in the gaps between two nanoparticles are also quite sensitive to the radius of the nanoparticles. The thickness of metal shell represents the distance over which this interaction takes place. The plasmon coupling strength between the core (hollow in nanoshell) and nanometal modes vanishes over the shell thickness d similar to the decay of the plasmonic field in the interparticle gap of the particle-pair system. In the nanoshell system, we can expect the fractional shift of the dipolar resonance to be a function of d, where d is the shell thickness. In other words, a larger hollow has a larger polarizability and a thinner shell ensures stronger near-field coupling, thus leading to a larger fractional plasmon shift. On the basis of our simulations, we set the shell thickness $d = 10$ nm. When a solid-silver nanodimer (case 1) is illuminated by incident light, the oscillating electric field causes the conduction electrons to oscillate coherently. When the electron cloud is displaced relative to the nuclei, a restoring force arises from Coulomb attraction between electrons and nuclei that results in oscillation of the electron cloud relative to the nuclear framework. The oscillation frequency is determined by four factors: the density of electrons, the effective electron mass, the shape and size of the charge distribution. The collective oscillation of the electrons is called the dipole plasmon resonance of the particle to distinguish from plasmon excitation that can occur in bulk metal or metal surfaces. Higher modes of plasmon excitation can occur, such as the quadrupole mode where half of the electron cloud moves parallel to the applied field and half moves antiparallel. Compared to the silver-shell nanodimer (case 2), more regions of positive and negative charge pair accumulations are located at inner and outer corners and adjacent sides.

First, we investigate the difference of the SCSs and near-field intensities as a function of wavelength on cases 1 and 2 which are illuminated with a TM

electromagnetic plane wave. SCS indicates the amount of light scattered in the far field. Figure 2a–d show the simulation results of the SCS and near-field intensities of cases 1 and 2 as a function of wavelengths of incident light. For the spherical case as shown in Fig. 2a, it can be clearly seen that a resonance peaks corresponding to the SPR mode can be found at $\lambda = 406$ nm. An obvious red-shift and SCS enhancement occurred in case 2 of spherical case when a solid-silver nanodimer is replaced by a silver-shell one, and the corresponding peak resonance of SPR is at $\lambda = 548$ nm. Note that the near-field intensity has the same tendency as SCSs as shown in Fig. 2e. Compared to the similar cases of ellipse, cone and box as shown in Fig. 2b–d, e–g, an obvious red-shift also occurred when case 1 is replaced by case 2, and both the position of SCS peaks and the near-field intensities of case 2 are higher than those of case 1. The corresponding TM-mode near-field distributions in cases 1 and 2: (a) $\lambda = 406$ nm for a solid spherical dimer, (b) $\lambda = 548$ nm for a nanoshell spherical dimer, (c) $\lambda = 440$ nm for a solid elliptical dimer, (d) $\lambda = 580$ nm for a nanoshell elliptical dimer, (e) $\lambda = 450$ nm for a solid triangular dimer, (f) $\lambda = 548$ nm for a nanoshell triangular dimer, (g) $\lambda = 530$ nm for a solid boxy dimmer and (h) $\lambda = 600$ nm for a nanoshell boxy dimer are depicted in Fig. 3. It can be clearly seen from Fig. 3 that the near-field distributions and edge enhancement obtained form case 2 are larger than those of case 1. These phenomena can be explained by the combination of SPR and the hollow effects inside the nanodimer, and the excited SPRs cover a more extended region of positive and negative charge pairs. The drastic increase in the degree of red-shifting in this case is due to the results from the fact that the interaction is mediated by the electromagnetic near field, which increases rapidly toward the shell surface (inner and outer surfaces). This effect can be applied to nanoparticle-based sensing or nanoantenna applications (Chau et al. 2010).

As deduced from the previous simulation results, now we investigate the rotational effects on the same cases of ellipse, cone and box but rotating to an angle of 45° as shown in Fig. 4. In case 2 system with a rotating angle of 45°, the similar tendency of SCSs and much higher field enhancement than those obtained from case 1 can be also seen in Fig. 5. Compared to the results of non-rotating cases (see
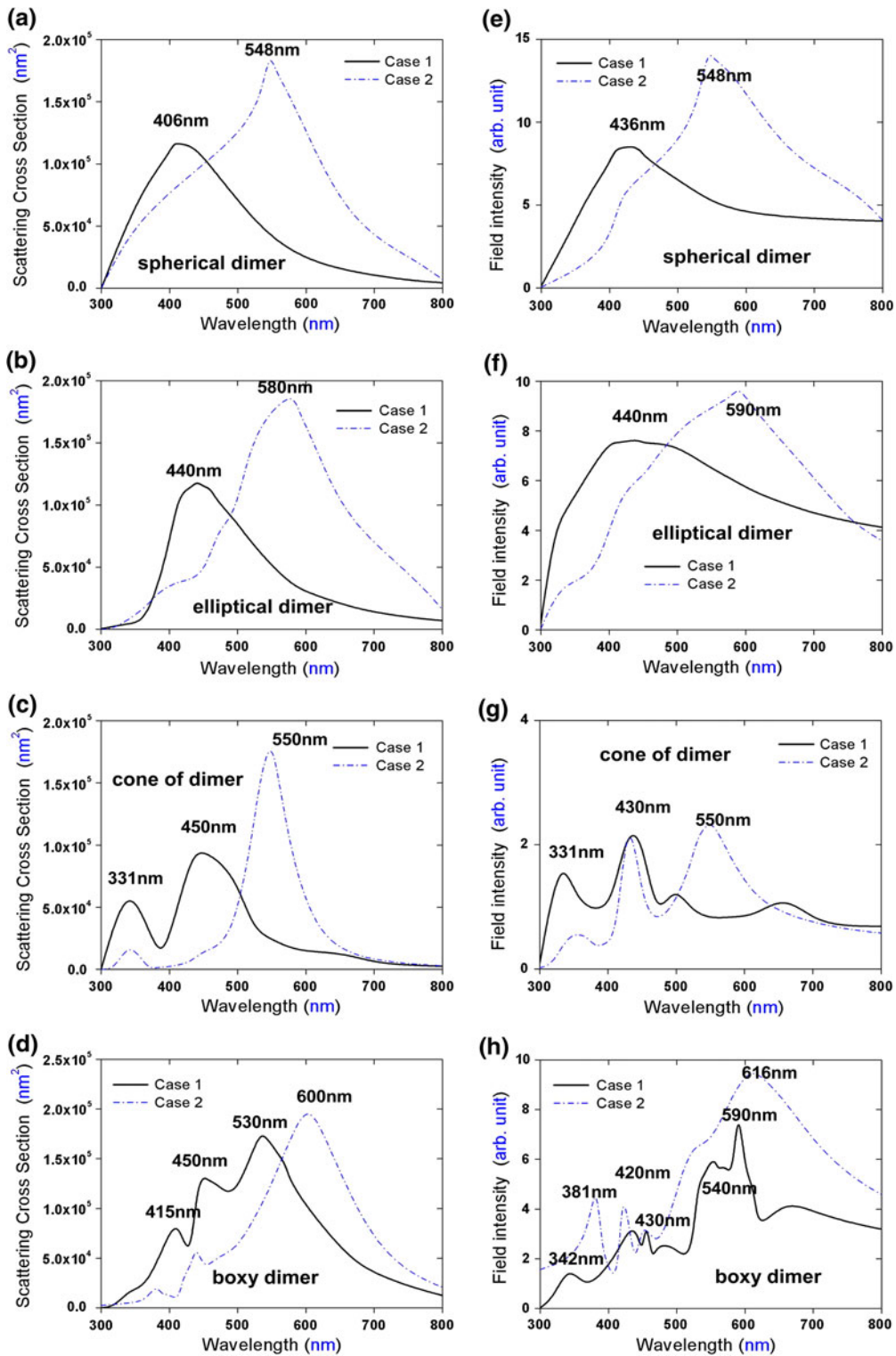
Fig. 2 a–d Scattering cross sections of cases 1 and 2 as a function of wavelengths of incident light. e–h Near-field intensities of cases 1 and 2 as a function of wavelengths of incident light
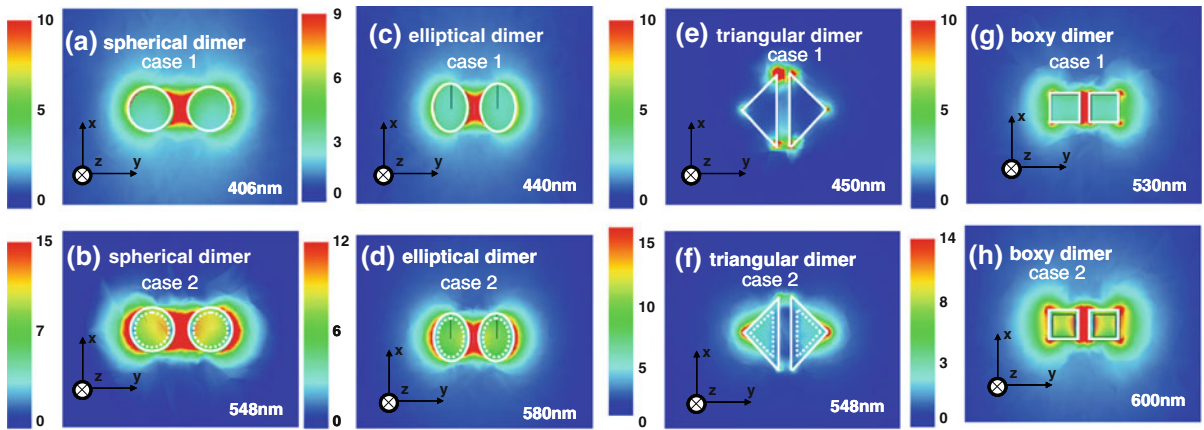
Fig. 3 Corresponding TM-mode near-field distributions in cases 1 and 2: **a** $\lambda = 406$ nm for a solid spherical dimer, **b** $\lambda = 548$ nm for a nanoshell spherical dimer, **c** $\lambda = 440$ nm for a solid elliptical dimer, **d** $\lambda = 580$ nm for a nanoshell elliptical dimer, **e** $\lambda = 450$ nm for a solid triangular dimer, **f** $\lambda = 548$ nm for a nanoshell triangular dimer, **g** $\lambda = 530$ nm for a solid boxy dimmer and **h** $\lambda = 600$ nm for a nanoshell boxy dimer
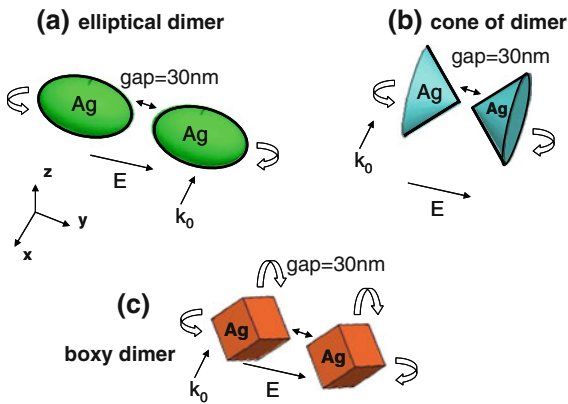

Fig. 4 Three patterns of simulation models: **a** elliptical, **b** cone of and **c** boxy rotational nanodimers with the same volumes $V = 1,046,666$ nm^3

Fig. 2f–h), the near-field intensities of rotational cases as shown in Fig. 5d–f are much higher than those of non-rotating cases. These cases are like nanoscale or nanoshell dipole nanoantennas (Chau et al. 2010), intense and opposite charge distributions accumulate at the facing edges when the field is polarized along the main axis. The SCSs and near-field intensities observed in Fig. 5a–f are directly related to the charge amount accumulated along the sides and the facing corners (or edges) of the silver-shell nanodimer (case 2). In molecular physics the interactions are usually expressed in terms of coupled multipolar moments (Kottmann and Martin 2001). In a same manner, the electronic response of plasmonic

nanoparticles can be expanded as a series of electric multipoles and can be used to design structure with optimized radiative losses, for example, by controlling the magnitude of the induced dipole moment.

The corresponding TM-mode near-field distributions for rotational cases, i.e., (a) $\lambda = 480$ nm for elliptical case 1, (b) $\lambda = 585$ nm for elliptical case 2, (c) $\lambda = 471$ nm for cone of case 1, (d) $\lambda = 560$ nm for cone of case 2, (e) $\lambda = 496$ nm for boxy case 1, and (f) $\lambda = 560$ nm for boxy case 2 are depicted in Fig. 6. In case 1, the high local-field enhancements appear in the vicinity of the solid-silver nanodimer and light is confined effectively in the gap of the pair due to the surface plasmon excitation. The field localization in the gap of a solid-silver nanodimer is determined by the polarization direction of the electric field of the incident light. For a single-pair system, the local field vanishes in the gap of the nanocylinder pair when the direction of the incident electric field is perpendicular to the major axis of the pair. Turning to the silver-shell nanodimer, the strong electromagnetic coupling between the inner and outer shell walls when the thickness ($d = 10$ nm) is small compared to the nanocylindrical radius.

Conclusion

Numerical investigations based on the FEM have been carried out to 3-D solid-silver nanodimer and silver-shell nanodimer of various geometries that
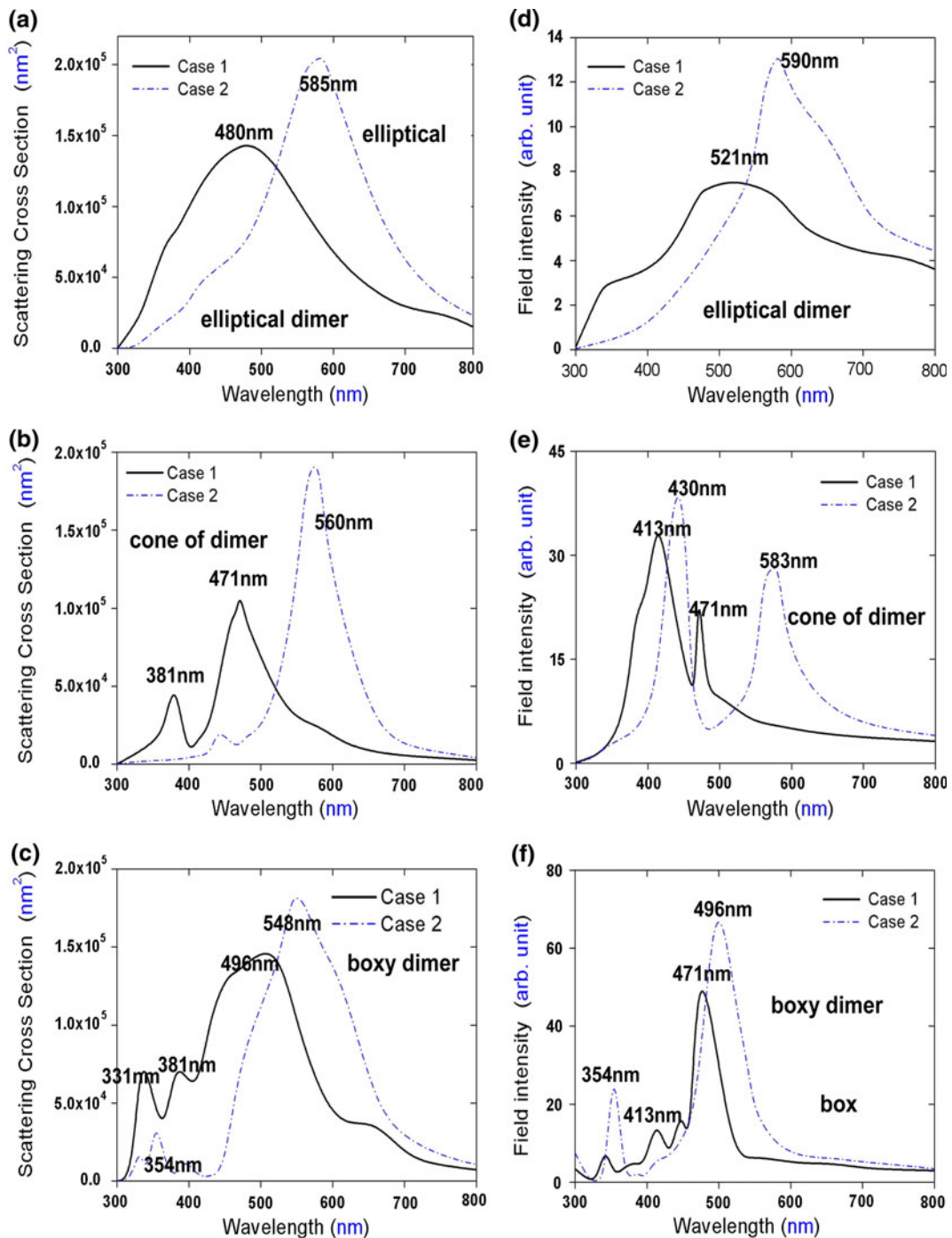
Fig. 5 a–c SCSs of rotational cases 1 and 2 as a function of wavelengths of incident light. **d–f** Near-field intensities of rotational cases 1 and 2 as a function of wavelengths of incident light

interact with incident plane wave of transverse magnetic polarization. The SCSs and near-field intensities are obtained as a function of wavelength.

Results show that the silver-shell nanodimer exhibits tunable SPRs in the near-field zone that are not observed for the solid cases with the same volumes.
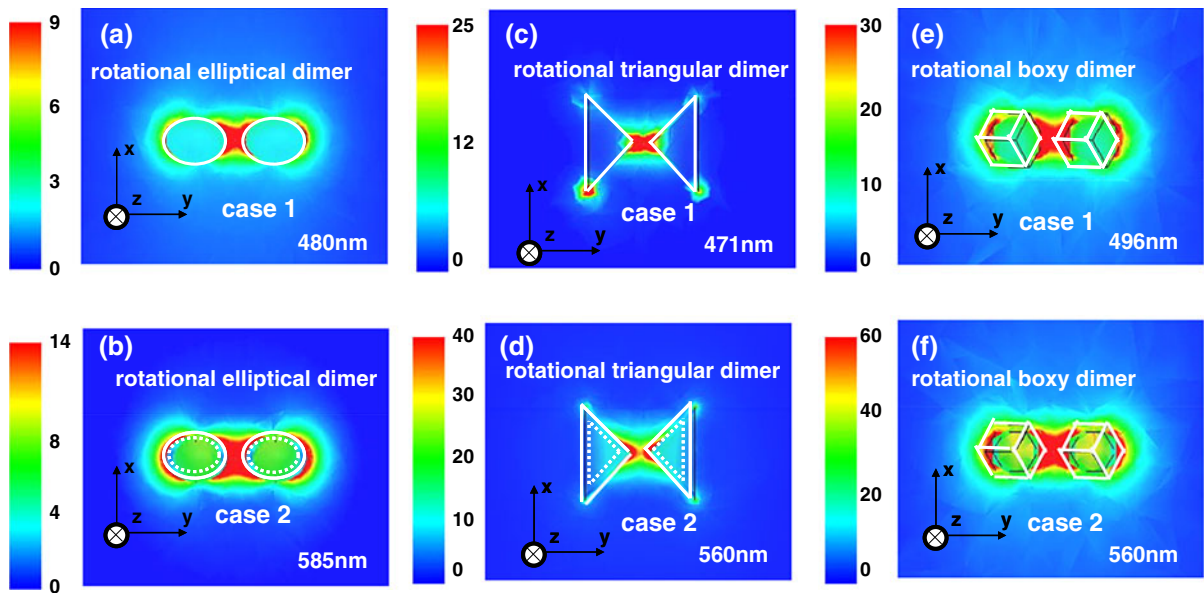
Fig. 6 Corresponding TM-mode near-field distributions for rotational cases, i.e., **a** $\lambda = 480$ nm for elliptical case 1, **b** $\lambda = 585$ nm for elliptical case 2, **c** $\lambda = 471$ nm for cone of case 1, **d** $\lambda = 560$ nm for cone of case 2, **e** $\lambda = 496$ nm for boxy case 1, and **f** $\lambda = 560$ nm for boxy case 2

Besides, it is also found that the rotational effects of silver-shell cases can induce more SPRs than the solid-silver cases in a wider range of wavelength. This effect can be applied to nanoparticle-based sensing or nanoantenna. In addition, the electronic response of plasmonic nanoparticles can be expanded as a series of electric multipoles and can be used to design structure with optimized radiative losses, for example, by controlling the magnitude of the induced dipole moment.

References

Averitt R, Sarkar D, Halas N (1997) Plasmon resonance shifts of Au-coated Au$_2$S nanoshells: insight into multicomponent nanoparticle growth. Phys Rev Lett 78:4217–4220

Chau YF, Tsai DP (2007) Three-dimensional analysis of silver nano-particles doping effects on super resolution near-field structure. Opt Commun 269:389–394

Chau YF, Yeh HH, Tsai DP (2008) Near-field optical properties and surface plasmon effects generated by a dielectric hole in a silver-shell nanocylinder pair. Appl Opt 47:5557–5561

Chau YF, Yeh HH, Tsai DP (2010) A new type of optical antenna: plasmonics nanoshell bowtie antenna with dielectric holes. J Electromagn Waves Appl 24:1621–1632

Chen C, Loo J, Deng M, Ronald K, Roeland H, Carmen B, Guido M, Gustaaf B (2009) Hollow platinum nanoshell tube arrays: fabrication and characterization. J Phys Chem C 113:5472–5477

Gresho PM, Sani RL (2000) Incompressible flow and finite element method, vol 1, 2. Wiley, New York

Hu Y, Fleming CR, Drezek RA (2009) Optical properties of gold-silica-gold multilayer nanoshells. Opt Express 16:19579–19591

Husu H, Canfield BK, Laukkanen J, Bai B, Kuittinen M, Turunen J, Kauranen M (2008) Chiral coupling in gold nanodimers. Appl Phys Lett 93:183115–183118

Johnson PB, Christy RW (1972) Optical constants of the noble metals. Phys Rev B 6:4370–4379

Kottmann J, Martin O (2001) Plasmon resonant coupling in metallic nanowires. Opt Express 8:655–663

Kottmann JP, Martin OJF, Smith DR, Schultz S (2000) Spectral response of plasmon resonant nanoparticles with a non-regular shape. Opt Express 6:213–219

Marty R, Baffou G, Arbouet A, Girard C, Quidant R (2010) Charge distribution induced inside complex plasmonic nanoparticles. Opt Express 18:3035–3044

Okamoto T, Kawata S (2001) Near-field optics and surface plasmon polaritons. Springer, Berlin, p 99

Oubre C, Nordlander P (2005) Finite-difference time-domain studies of the optical properties of nanoshell dimmers. J Phys Chem B 109:10042–10051

Prodan E, Radloff C, Halas NJ, Nordlander P (2003) A hybridization model for the plasmon response of complex nanostructures. Science 302:419–422

Quinten M, Leitner A, Krenn J, Aussenegg F (1998) Electromagnetic energy transport via linear chains of silver nanoparticles. Opt Lett 23:1331–1333

Zhou S, Honma HSI, Komiyama H (1994) Controlled synthesis and quantum-size effect in gold-coated nanoparticles. Phys Rev B 50:12052–12056